Multiuser-MIMO Transmitter Based on Optical Polar-Vector Modulators

Garrett J. Schneider, Janusz A. Murakowski, Shouyuan Shi, Munawar Kermalli, Stefano Galli, *Fellow, IEEE*, Xiao-Feng Qi, and Dennis W. Prather, *Senior Member, IEEE*

***Abstract*— We present the use of a novel optical modulator architecture to achieve simultaneous radiofrequency (RF) multi-user beamforming and data modulation. Optical vector modulators enable control of the complex state of a transmitted wave by directly and independently controlling both amplitude and phase. Operating in the optical domain affords extremely wide bandwidth and negligible dispersion in such modulators. A demonstration experiment is presented based on a 2-element transmit array, where the vector modulators were assembled from pairs of commercial phase and amplitude modulators. The results of the experiment show independent data directed into two different spatial beams simultaneously, using the same RF carrier.**

***Index Terms*— Microwave photonics, MIMO, electro-optic modulators, wireless communication.**

I. Introduction

THE incorporation of spatial diversity within wireless communications networks, generally referred to as multiple-input/multiple-output (MIMO), has advanced in a progression from single-user (SU) MIMO systems, where spatial diversity is introduced to render a more robust communication channel [1], to multi-user (MU) MIMO, where beam-space concepts are introduced to provide enhanced data capacity through parallel data transmission [2]. In both cases, pre-coding techniques can be used to account for channel-state information (CSI) and render a more effective overall communication system. The progression continues today toward so-called massive MIMO [3], where a very large number of antennas is used to exploit the spatial diversity of the channel state to serve multiple users within the same frequency resource allocation. However, as the beam-space dimension increases, the generated field over a radiating aperture approaches a continuum of plane waves with associated complex weights (with CSI also encoded as an additive set of complex weights), and the required complex wave amplitude across the aperture becomes a holographic profile. Moreover, this radiofrequency (RF) hologram must be regenerated synchronously over the aperture at the highest transmitted symbol rate.

Manuscript received June 8, 2018; revised July 12, 2018; accepted August 15, 2018. Date of publication August 31, 2018; date of current version November 6, 2018. *(Corresponding author: Dennis W. Prather.)*

Invited paper for the Integrated Microwave Photonics Special Issue.

G. J. Schneider, J. A. Murakowski, S. Shi, and D. W. Prather are with the University of Delaware, Newark, DE 19716 USA, and also with Phase Sensitive Innovations, Inc., Newark, DE 19713 USA (e-mail: gschneid@udel.edu; jam@udel.edu; sshi@udel.edu; dprather@udel.edu).

M. Kermalli, S. Galli, and X.-F. Qi are with FutureWei Technologies, Inc., Bridgewater, NJ 08807 USA (e-mail: munawar.kermalli@huawei.com; stefano.galli@huawei.com; xiao.feng.qi@huawei.com).

Digital Object Identifier 10.1109/LPT.2018.2868248

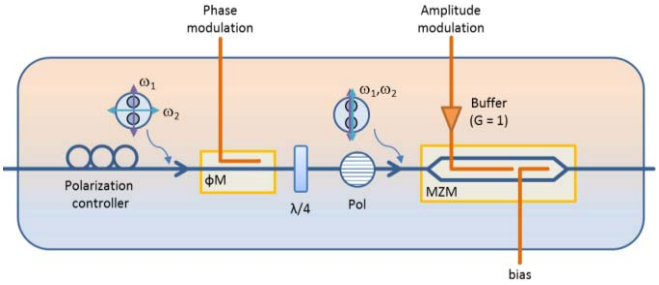

Fig. 1. Schematic diagram of the vector modulator as implemented. MZM: Mach-Zehnder (intensity) modulator; ΦM: phase modulator; Pol: linear polarizer; $\lambda/4$: quarter-wave plate.

To implement such a transmit (Tx) aperture, namely, one capable of radiating holographic wave amplitude profiles, requires a dense array of transmitting elements that have continuous amplitude and phase control over the entire communication bandwidth, such that the far-field radiation pattern becomes optimally matched to the overall requirements of the communication system. Such control can be achieved over extremely wide operating bandwidths using photonic components, namely electro-optic modulators, to generate and process RF communications signals in the optical domain.

In this letter, we propose what we call optical polar-vector modulators (or simply "vector modulators" for brevity) for implementing the holographic array just described, and we describe a simple two-channel MIMO proof-of-concept experiment demonstrating their operation and capabilities. The experimental results establish that such modulators can be used to realize a wideband holographic MU-MIMO transmitter.

II. Experiment Design

A. Two-Channel Tx System Using Polar-Vector Modulators

A two-element photonic Tx array was constructed as follows. A tunable optical paired-laser source (TOPS) was used to generate coherent offset optical beams [4], which were combined in a fiber-based polarization beam combiner. The combined output comprised the two laser wavelengths conveyed in a single polarization-maintaining (PM) fiber, with one wavelength in each of the fiber's linear transverse polarization modes. This was next fed through a 50/50 splitter, and subsequently to a pair of vector modulators, depicted schematically in Fig. 1.

Each vector modulator was assembled from a pair of commercial lithium niobate (LN) modulators, one phase-only

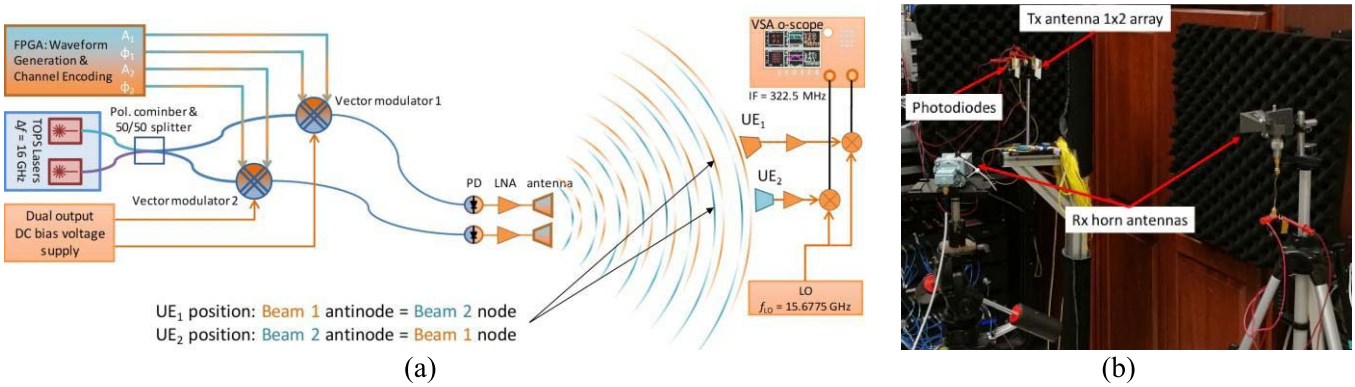

Fig. 2. (a) Illustration of the spatial beam arrangement of the multi-beam Tx configuration. Each of the two beams is formed by the combination of both antennas. Signals from the FPGA drive the modulators such that each beam conveys independent data to one of the two user equipment (UE) locations. (b) Photograph of the demonstration setup showing two Tx antennas and two Rx antennas.

and one Mach-Zehnder Interferometer (MZI) amplitude, along with polarization-control components. The vector modulators are preceded by polarization controllers to optimize the input coupling to the phase modulator and minimize unintended amplitude modulation arising from contamination of the modulator's polarization modes with both laser wavelengths. With proper alignment, one laser wavelength is inserted into each of the phase modulator's transverse modes, which interact with the drive voltage via different components of the LN electro-optic matrix, and thereby impose a different phase shift onto the two wavelengths [5], [6]. This phase offset is preserved upon downconversion at a photodiode detector, whereas fiber-induced optical phase variations affect both wavelengths identically and have no effect.

Following the phase modulator, the optical beams pass through optical components to project the two wavelengths onto a common polarization mode. Specifically, a free-space cascade of a ¼-wave plate and a linear polarizer is used to first convert both wavelengths from linear to circular, then to project them both onto vertical linear polarization (incurring a 3-dB loss) and launch them back into PM fiber. Next follows the MZI amplitude modulator which affects the amplitude of both wavelengths identically since they are now both in a common polarization mode. The MZI modulator outputs are fed to photodiodes, where the wavelengths mix and downconvert to RF for transmission via a pair of antipodal Vivaldi antennas. Transmitted signals are received by simulated user equipment (UE) comprised of single horn antennas. Figure 2 illustrates the described experimental configuration.

B. Signal Encoding

Each beam is simultaneously formed from the output of both Tx elements, such that one data stream interferes constructively at the same location where the other stream interferes destructively, and vice versa. This means that separate Rx antennas placed at the correct locations will each receive only one data stream, whereas at other positions, both streams will be present and their interference will render the signals unrecoverable. Thus, the same pair of vector modulators does both beam forming and data encoding simultaneously.

The signals which drive the vector modulators are provided by a National Instruments FPGA-based real-time I/O system. Signals comprising pseudorandom sequences of digital data were pre-computed and loaded into FPGA memory. Quadrature-amplitude modulation (QAM) symbols were mapped from a basis of separate beams for each UE into the Tx antenna basis by a 2×2 beam-space encoding matrix. Generally, in massive MIMO the channel-state matrix must be obtained using pilot measurements and reciprocity, and updated periodically to account for changes in the environment, but in the case of this demonstration, we assumed ideal, fixed channel conditions and analytically calculated the simple 2×2 matrix required to ensure that each beam's maxima were co-located with the other's minima. Because there are only 2 Tx antennas, it is not possible to orthogonalize the beams for arbitrary UE positions. Next, these complex values were decomposed into their amplitude and phase components (i.e. polar coordinates in the complex plane, as opposed to the conventional Cartesian system of I-Q modulation; hence the designation 'polar-vector'). Finally, the transformed data vectors are scaled by the modulators' measured V_π values and converted to analog outputs, to impart QAM modulation onto the transmitted RF beams. Figure 3 illustrates this encoding process.

C. Experimental Setup

The TOPS source was configured to offset the laser wavelengths by 16 GHz, hence this was the RF carrier frequency used. The photodiodes were commercial packages from u^{2}t Photonics (now Finisar). Each photodiode was illuminated by about 0.4 mW of optical power, generating about 0.3 mA of DC photocurrent. The Vivaldi antennas were attached to the photodiode packages' coaxial output connectors, and were positioned about 4 cm apart. The receive (Rx) antenna was a ~15-dB gain horn placed at a distance of about 2 m from the transmitters. The horn output was fed to a low-noise amplifier (LNA) with 33-dB gain and 3-dB noise figure. The signals were received and data constellations recovered using a combination of a mixer with IF output at 322.5 MHz, and a Keysight oscilloscope running vector signal analysis (VSA) software. The FPGA was set up to drive the modulators at a symbol rate of up to 200 kHz. Phase modulators were driven directly by the FPGA hardware through their high-impedance bias electrodes. Due to the 50-ohm impedance of the MZI modulators' RF inputs, unity-gain buffer amplifier circuits were assembled and installed between the FPGA and the modulators to provide sufficient current to drive them at

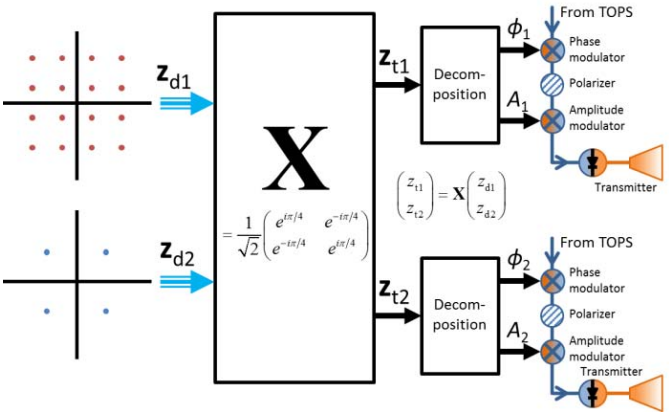

Fig. 3. Diagram of the data encoding scheme. Data streams are constructed as vectors of complex numbers (z_{d1} & z_{d2}) taken from the discrete set contained within the constellation corresponding to a chosen QAM modulation. The channel encoding matrix X shown maps the data streams from the UE basis into the Tx element basis (z_{t1} & z_{t2}). These transformed complex values are decomposed into amplitude and phase components, and after scaling by the modulators' drive voltages, the signals are output from the FPGA to the vector modulators.

the required levels. Variable DC power supplies were used to adjust the MZIs for quadrature biasing.

III. Experiment Results

A. Two-Beam Continuous Tx Demonstration

Two different two-beam configurations are presented here, each configuration generating two spatial beams carrying different data encoded with different modulations, enabling the two signals to be easily distinguished at the receiver. In the first configuration, the data streams were both encoded as 4-QAM (QPSK), but with different symbol rates in a ratio of 2:1. In the second, the two beams' symbol rates were the same, but one beam was encoded as 4-QAM while the other was encoded as 16-QAM. No band-limiting filter was applied to the computed output waveforms. Figure 4 contains VSA screen captures of recovered data constellations for the two different 2-beam configurations. It is clear from the data shown that the 2-element vector-modulator scheme has successfully generated 2 independently modulated spatial beams simultaneously.

The results shown in Fig. 4 were obtained serially, with a single Rx antenna that was repositioned between the measurements of each beam. Later, we added a second Rx antenna and downconversion mixer that allowed us to recover data from both beams simultaneously. The RF carrier frequency was reduced to 13 GHz to accommodate the second antenna. A screen capture from this configuration is shown in Fig. 5. The recovered SNRs are similar to those seen in the data of Fig. 4: 15.0 dB for the 4-QAM beam, and 18.1 dB for 16-QAM.

Several factors contribute to signal distortions in this experiment. The dominant contribution arises as a consequence of the fact that with only two Tx elements, the nulling of one beam at the location of the other is extremely sensitive to the beams' pointing directions and the amplitude balance between the two elements. The pointing direction tends to vary/drift slowly, likely caused by thermal drift in the phase modulators. It can be corrected with a small bias voltage,

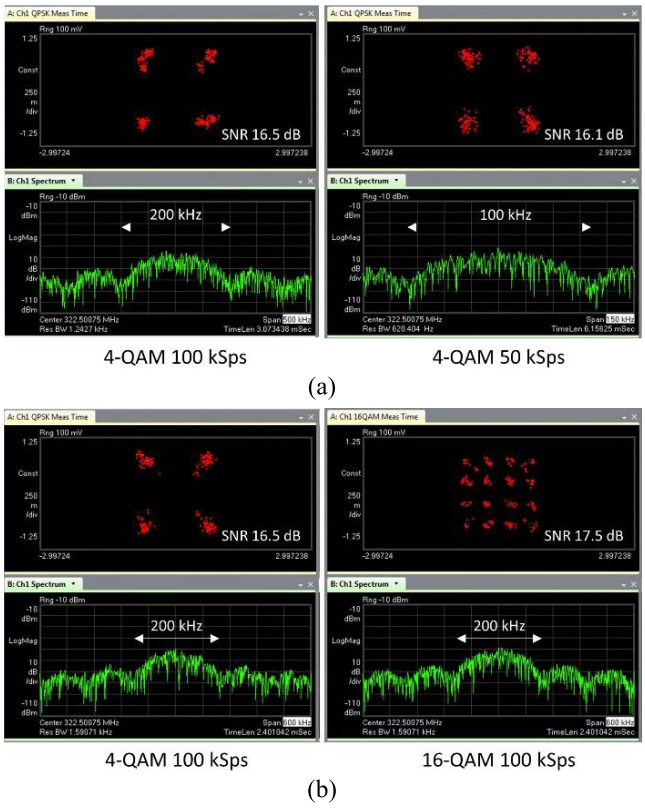

Fig. 4. Recovered constellations and spectra from the multibeam Tx demonstration experiment. (a) First beam configuration: Beam 1 was 4-QAM at 100 kSym/s, beam 2 was 4-QAM at 50 kSym/s. Note the spectra in this pair of images are plotted with different spans. (b) Second beam configuration: Beam 1 was 4-QAM at 100 kSym/s, beam 2 was 16-QAM at 100 kSym/s.

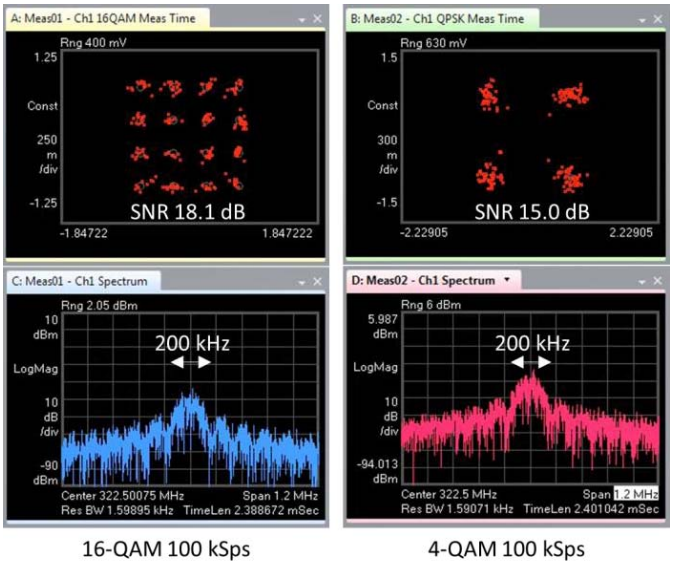

Fig. 5. VSA screen capture from two Rx antennas positioned in the two beams, recovering independent data streams simultaneously. Left (right) column shows constellation and spectrum for 16-QAM (4-QAM) beam. The symbol rate for both beams was 100 kHz.

but in the work presented here we did not have the means to continuously monitor and control this drift. The amplitude balance also tends to drift very slowly over time as the temperature of the TOPS's internal components changes. It can be adjusted by optical attenuation at the inputs

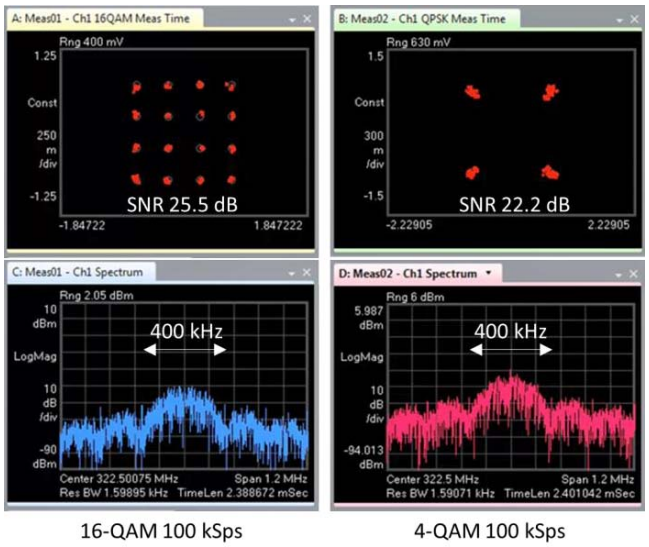

Fig. 6. VSA screen capture from two time-multiplexed simultaneously transmitted beams. Compared to the results of Fig. 5, these constellations exhibit much better SNR, but the transmitted bandwidths of the beams is double that shown in Fig. 5, although the symbol rate is the same in both cases.

to the photodiodes. Another likely cause of signal degradation is the fact that the symbol rates in both beams are identical and synchronous, so the cross-talk between the beams is highly correlated with the intended data. Improvements can be realized by structuring/timing each data stream such that any cross-talk appears more like random noise, e.g. by off-setting the symbol-to-symbol transitions in time and/or using different symbol rates. Alternatively, the beams can be time-multiplexed, such that only one beam is transmitted at any instant. While not formally MIMO, such a configuration is effective at reducing spatial interference, particularly for the crude beams that can be formed from only two array elements.

B. Symbol-Rate Time-Multiplexing Demonstration

An alternative approach to realizing the goal of transmitting multiple independent spatial beams from a common aperture and on a common carrier signal, namely time multiplexing user data at (or above) the symbol rates being transmitted to the various users, has also been demonstrated. This approach is in contrast to the one just presented, where all beams are transmitted continuously to all users.

A drawback of the continuous-transmission approach is that the total transmitted power is divided among the users, while any imperfection in the spatial isolation between the beams results in interference, degrading the beams at both the upper and lower ends of their power range. Alternatively, the time-multiplexing approach uses the speed and flexibility of the vector modulators to generate a new, custom beam each time a symbol is updated for any user's data, where the beams formed instantaneously address only one of the users at a time (or perhaps a small subset of all users in the case of many users), using all the power available and without the possibility of cross-talk from other beams being transmitted at the same time. In the present two-user demonstration, each symbol is transmitted to its designated UE for only half the duration of the continuous beam case, but the greatly improved SNR more than compensates. However, this configuration doubles the bandwidth used to transmit the same symbol rate. This cross-talk reduction is readily apparent in the simultaneously recovered signal constellations shown in Fig. 6, showing measured SNR to be >7 dB better than the results depicted in Fig. 5: 25.5 dB for 16-QAM, and 22.2 dB for 4-QAM.

IV. Conclusions

An optical polar-vector modulator concept has been proposed and demonstrated in a two-element, two-beam MU-MIMO proof-of-concept experiment. The experimental demonstration used a single set of vector signals applied to an array of modulators to do both beamforming and data modulation simultaneously. This is akin to full digital beamforming approaches, except that in this case the RF carrier is embedded in a coherent tunable-offset laser pair, and synchronization across all the array elements is achieved automatically since the same laser pair drives all elements. Operating in the optical domain, the vector modulators possess enormous bandwidth and negligible dispersion, allowing them to operate at high speeds. Implemented in a large, dense array, this architecture enables the formation of dynamic RF holograms that can be updated at speeds greatly exceeding the baud rates used in wireless communications, limited in principle only by the speed of the digital-to-analog converters generating the baseband data.

Looking forward, the proposed and demonstrated Tx architecture can be implemented with broadband, integrated, optically fed, high-power photodiode driven antenna arrays [7], [8], and coupled with a photonically enabled beam-space beamforming receiver [9], [10] that can provide real-time analog CSI from UE pilots via imaging, to realize a powerful, practical solution for massive MIMO.

References

[1] A. J. Paulraj and T. Kailath, "Increasing capacity in wireless broadcast systems using distributed transmission/directional reception (DTDR)," U.S. Patent 5 345 599 A, Sep. 6, 1994.

[2] D. Gesbert, M. Kountouris, R. W. Heath, Jr., C.-B. Chae, and T. Sälzer, "Shifting the MIMO paradigm," *IEEE Signal Process. Mag.*, vol. 24, no. 5, pp. 36–46, Sep. 2007.

[3] T. L. Marzetta, "Noncooperative cellular wireless with unlimited numbers of base station antennas," *IEEE Trans. Wireless Commun.*, vol. 9, no. 11, pp. 3590–3600, Nov. 2010.

[4] G. J. Schneider, J. A. Murakowski, C. A. Schuetz, S. Shi, and D. W. Prather, "Radiofrequency signal-generation system with over seven octaves of continuous tuning," *Nature Photon.*, vol. 7, pp. 118–122, Feb. 2013.

[5] S. Shi *et al.*, "Conformal wideband optically addressed transmitting phased array with photonic receiver," *J. Lightw. Technol.*, vol. 32, no. 20, pp. 3468–3477, Oct. 15, 2014.

[6] J. Bai *et al.*, "Optically driven ultrawideband phased array with an optical interleaving feed network," *IEEE Antennas Wireless Propag. Lett.*, vol. 13, pp. 47–50, 2014.

[7] M. R. Konkol *et al.*, "High-power photodiode-integrated-connected array antenna," *J. Light. Technol.*, vol. 35, no. 10, pp. 2010–2016, May 2017.

[8] F. Wang *et al.*, "Photonic generation of high fidelity RF sources for mobile communications," *J. Light. Technol.*, vol. 35, no. 18, pp. 3901–3908, Sep. 2017.

[9] D. W. Prather *et al.*, "Optically upconverted, spatially coherent phased-array-antenna feed networks for beam-space MIMO in 5G cellular communications," *IEEE Trans. Antennas Propag.*, vol. 65, no. 12, pp. 6432–6443, Dec. 2017.

[10] J. C. Deroba, G. J. Schneider, C. A. Schuetz, and D. W. Prather, "Multi-function radio-frequency photonic array with beam-space down-converting receiver," *IEEE Trans. Aerosp. Electron. Syst.*, to be published, doi: 10.1109/TAES.2018.2829359.